Time-resolved polarization lock-in filtering for background suppression in Raman spectroscopy of biomass pyrolysis

Kim, Haisol; Gong, Miaoxin; Kristensson, Elias; Ehn, Andreas; Aldén, Marcus; Brackmann, Christian

Published in:
Combustion and Flame

DOI:
10.1016/j.combustflame.2020.12.011

2020

Document Version:
Publisher's PDF, also known as Version of record

Combustion and Flame 224 (2021) 219–224

Contents lists available at ScienceDirect

Combustion and Flame

journal homepage: www.elsevier.com/locate/combustflame

Time-resolved polarization lock-in filtering for background suppression in Raman spectroscopy of biomass pyrolysis

Haisol Kim, Miaoxin Gong, Elias Kristensson, Andreas Ehn, Marcus Aldén, Christian Brackmann*

Division of Combustion Physics, Lund University, P.O. Box 118, SE-22100 Lund, Sweden

ARTICLE INFO

Article history:
Received 9 September 2020
Revised 4 December 2020
Accepted 4 December 2020
Available online 21 December 2020

Keywords:
Laser diagnostics
Raman spectroscopy
Polarization lock-in filtering
Biomass pyrolysis

ABSTRACT

Laser-based Raman spectroscopy is a powerful technique for non-intrusive measurements of chemical composition in gas, liquid, and solids. However, weak signals make it challenging to employ the technique for diagnostics under harsh conditions with various background interferences. To overcome such limitations, we have devised a method, polarization lock-in filtering (PLF) based on temporal modulation of the excitation laser polarization, to filter out polarization-independent signals from acquired data. The PLF method applied for continuous Raman spectroscopy measurements of a biomass pyrolysis process showed promising filtering abilities for unwanted background fluorescence signals. A broadband fluorescence background interference was suppressed by up to a factor of 50. Therefore, released species during the biomass pyrolysis process were readily identified with their Raman spectrum signatures and their amounts quantified. In addition, the PLF method provided Raman spectra of low background, from which a gradual change in hydrocarbons released at different stages during the pyrolysis could be observed. Altogether, the efficient background suppression method increases the general applicability of Raman spectroscopy under conditions where interfering signals present a challenge and a limiting factor.

1. Introduction

Chemical reaction processes, e.g., combustion, include rapid formation and decomposition of species together with large heat release. Such systems are very complex and sensitive, and thus *ex situ* gas-sampling methods for investigating gas compositions are challenging and associated with uncertainties related to the sampling process itself. On the other hand, laser-based diagnostic techniques can be utilized to investigate processes under harsh conditions with strong gradients without perturbing the studied phenomena. Raman spectroscopy is such a method that can detect multiple chemical species simultaneously, and the signal is proportional to the species concentration, making it quite straightforward to conduct quantitative analysis. However, Raman scattering is a relatively weak process compared to interactions utilized in other laser-based techniques. Therefore, despite its strong points, Raman spectroscopy is often opted out when there are various background sources at the probe volume, e.g., strong elastic scattering of laser light or fluorescence.

Nevertheless, Raman spectroscopy has been employed for combustion diagnostics since the 1970s [1–3], and a review of its development has been presented by Eckbreth [4]. Enhanced sensitivity for Raman spectroscopy can be realized using configurations with multiple passages of the excitation laser beam through the measurement region; an early example of a multipass cell for Raman spectroscopy of gases was presented by Hill and Hartley [5] while a later design demonstrated for studies in flame has been devised by Utsav et al. [6,7]. Raman measurements using continuous-wave lasers can be feasible under conditions with a low level of background light while diagnostics of luminous flames require gated detection and pulsed lasers, which also is necessary for studies under non-stationary conditions, e.g., in turbulent combustion. However, for lasers with high pulse energy operating at a low repetition rate, typically 10 Hz, the high irradiance obtained with a focused beam can induce electric breakdown and plasma formation. The subsequent broadband emission of the plasma then interferes with the acquisition of the weak Raman signal. One way to avoid this problem is to use pulse-stretcher concepts introduced by Nguyen et al. [8] and employed by many research groups [9–14]. The pulse is stretched temporally using multiple optical ring cavities or delay lines, and it was, for example, reported by Kojima and Nguyen that a pulse of duration 8.4 ns (FWHM) was expanded

* Corresponding author.
E-mail address: christian.brackmann@forbrf.lth.se (C. Brackmann).

https://doi.org/10.1016/j.combustflame.2020.12.011

to over 150 ns while maintaining 82% of its initial energy [9]. However, the downside with this type of setup is increased complexity in the optical arrangement. Alternatively, lasers with high repetition rates, e.g., 5 kHz, and lower pulse energies can be employed to achieve high average power (in the range between 10 and 100 W) and yet avoid problems with laser-induced plasma [15].

The detection sensitivity can also be improved by suppressing the background from stray light and thus achieve a higher signal-to-background ratio. A means to accomplish background suppression was introduced by a method called periodic shadowing (PS) [16]. Installing a Ronchi grating at the entrance slit of the spectrometer and creating an imprinted pattern on the signal, combined with a spatial lock-in filtering in the Fourier domain, results in an efficient suppression of background light that reached the detector from unwanted directions. In the previous study, the PS method was investigated with four different spectroscopic measurement techniques: emission, absorption, laser-induced scattering, and Coherent anti-Stokes Raman Spectroscopy (CARS). Depending on the type of technique and spectral region of interest, an improvement of the signal-to-background ratio by a factor from 20 to 300 was observed. The concept was especially helpful when multiple scattering in the vicinity of the probe volume presented a problem, and therefore, it was also implemented in our Raman spectroscopy setup to improve the detection sensitivity.

Even though the PS method is efficient for reducing the problem with multiple scattering, it, however, cannot filter out interfering laser-induced emission, e.g., fluorescence, originating from the probe volume. These interfering signals follow the same path through the detection system as the Raman signal and will thus not be suppressed with PS. In cases when such undesired background contributions are un-polarized, they can be subtracted from the polarized Raman signal by measurements at orthogonal detection polarizations [13,17–20]. While this can be readily achieved for investigations under static conditions, measurements on time-varying processes are often desirable. Simultaneous acquisition of signals with orthogonal polarizations can then be achieved with dual detection setups, for example, employed in studies of turbulent combustion [13]. As an alternative for studies of moderately time-varying processes, we devised a method, polarization lock-in filtering (PLF), based on a continuous change in polarization of the incident laser beam resulting in Raman signals modulated in time while un-polarized signals such as fluorescence remain unaffected. The acquired data modulated in time are post-processed using lock-in filtering, similar to the PS method. The novelty compared with the previous approach is the continuous mode of operation that allows processes varying on a second-scale to be followed in time with the retrieval of background-free spectra using a single detection system. The method is rather simple to implement experimentally but clearly extends the applicability of Raman spectroscopy for studies of time-varying processes.

This paper presents background suppression using the PS and PLF methods to address the challenges of background interferences in Raman spectroscopy under harsh measurement conditions. The combined PS and PLF methods were employed to investigate gas released from a biomass pyrolysis process, which is accompanied by the release of hydrocarbon volatiles [21] that, upon laser excitation, can result in strong fluorescence swamping Raman signals. This background prohibits analysis of gas composition both in terms of permanent gases, e.g., CO, CO_2, H_2, and CH_4, but also of its content of hydrocarbon volatiles and tars [21,22], which is an indicator of gas quality. Tar composition is dependent on the residence time of the tar-laden gas at high temperature as well as other operational conditions, see, e.g., [23]. While conventional adsorption methods for tar analysis can provide detailed information on their composition, they are time-consuming (~hours), making correlations with process changes and conditions challenging. Therefore, measurement techniques that enable *in situ* on-line measurements are of high value in the characterization of biomass conversion. In such studies, the combined background filtering techniques are very useful to retrieve Raman spectra with significantly reduced background and allow for identification and quantitative analysis of signals of carbon monoxide, hydrocarbons, and water.

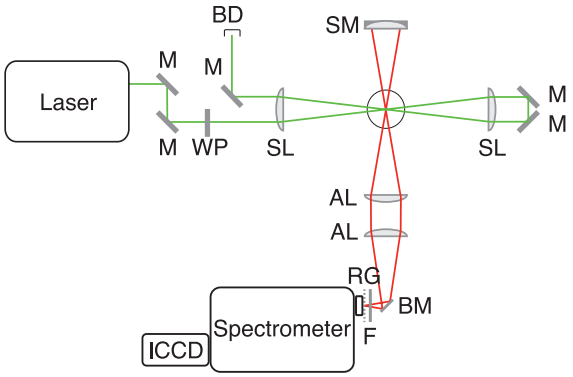

Fig. 1. Schematic of the experimental setup for Raman spectroscopy. The green line represents the laser beam while the red line represents the signal path. A double-pass setup was used to study a biomass pyrolysis process in the measurement volume indicated by a circle. Abbreviations: M – mirror, WP – half-wave plate, SL – spherical lens, SM – spherical mirror, BD – beam dump, AL – achromatic lens, BM – pair of broadband mirrors for image rotation, F – 532 nm long-pass filter, RG – Ronchi grating, and ICCD – intensified CCD camera. (For interpretation of the references to color in this figure legend, the reader is referred to the web version of this article.)

2. Methodology

2.1. Raman spectroscopy

An Nd:YAG laser (HD40I-OE, Edgewave, 100 W) operating at a repetition rate of 5 kHz was employed for Raman spectroscopy. The operating power of the laser was set to 25 W to prevent damaging optical components. A schematic of the experimental setup is shown in Fig. 1.

A double-pass arrangement consisting of two spherical lenses of $f = 200$ mm focal length and planar dichroic mirrors was used for the laser beam to pass through the measurement volume twice while being focused at the common intersection where the crossing angle between the beams is 8°. A pellet bed, explained more in the following section, was located right below the measurement volume.

A portion of the scattering signal from the probe volume was collected into an $f = 320$ mm spectrometer (IsoPlane SCT 320, Princeton Instruments) using two achromatic lenses of focal length $f = 200$ mm. Between the set of lenses and the spectrometer, a pair of broadband aluminum mirrors was placed in an arrangement that rotates the image of the probe volume by 90° to match the orientation of the slit. The spatially resolved Raman signal for a 6 mm distance along the laser beams was recorded on the CCD sensor, and the spatial resolution was estimated to be 80 µm. A long-pass filter (532 nm EdgeBasic^{TM}, Semrock, OD7) was positioned at the slit to suppress elastic scattering and straylight at the laser wavelength, and no appreciable contributions were observed in the spectral regions of the vibrational Raman peaks. The spectrometer was equipped with three different gratings with 600, 1800, and 2400 lines/mm allowing for measurements with different spectral resolution. Depending on the spectral region of interest and purpose of the measurement, different gratings were used to study a particular spectral range in detail or to acquire a full spectrum. The results presented in this paper were recorded with the 600 lines/mm grating, centered at wavelength 627 nm. The

spectrally dispersed signal from the spectrometer was recorded on an intensified CCD camera (PI-MAX 4, GEN III, Princeton Instruments) with an intensifier gate width of 30 ns to suppress continuous background. Raman signals generated by 2000 pulses were accumulated into one image, with an acquisition time of 0.4 s, to enhance the signal-to-noise ratio. Such accumulated images were recorded continuously during measurements with a frame rate of 1.86 fps for 330 s.

2.2. Periodic shadowing and polarization lock-in filtering method

The periodic shadowing (PS) method was implemented by installing a Ronchi grating, denoted RG in Fig. 1, on the entrance slit of the spectrometer. A stripe pattern of 5 lines/mm printed on the grating alternately blocks and transmits signal entering the spectrometer. Only light that has propagated through the entrance slit and followed its intended path inside the spectrometer will preserve the periodic pattern and create a spatially modulated image on the CCD chip. Thus it is possible to filter out stray light by digital lock-in amplification in the post-processing. Subsequent binning of each image vertically results in a Raman spectrum, filtered from interfering stray light, that can be further analyzed in the same manner as an ordinary Raman spectrum. For a more detailed explanation of the PS method, readers are referred to the work of Kristensson et al. [16]. In this study, results were obtained for measurements with combined PS and PLF methods. However, the focus of the discussion is on the PLF method with comparisons of data before and after applying the PLF processing.

For the PLF method, a half-wave plate, denoted WP in Fig. 1, was manually rotated from 0 to 45° and back, which changed the polarization of the incident beam from vertical to horizontal and back to the vertical orientation continuously at a frequency of 0.5 Hz. Therefore, the intensity of polarization-dependent signals, e.g., Raman scattering, varied periodically with time in the set of data. In the two-dimensional data set with the wavelength on the x-axis and time on the y-axis, a periodicity is imprinted along the time direction due to the variation, and it is equivalent to the spatial periodic pattern imprinted on the signal in the PS method. The data with the periodicity was then Fourier filtered to only retain components with the frequency of the modulation. With this filtering method, continuous measurements are possible, and it is not required to precisely synchronize the timing of the polarization shift and the recording. The temporal modulation pattern of the signal resembled a square-wave, and the filtering process resulted in a signal reduction of ~30% while the spectral shape was preserved after processing. Thus, the processed data show a dynamic range equal to ~70% of the detector range.

In this study, it was assumed that Raman signals are completely polarized whereas background signals are assumed to be polarization-independent. However, for more accurate quantification, depolarization ratios of molecules need to be included, and it can result in an error of 10% at a maximum when this is neglected. In addition, background levels are not fully polarization-independent due to the properties of molecules and polarization-dependency of optical components in the measurement setup. For example, the laser power was measured at the end of the beam path for different polarization orientations, and the horizontal polarization showed 2% decrease compared with the vertical polarization. This intensity drop can be compensated for in the data processing when accurate quantification is wanted.

2.3. Biomass pellet and pellet bed

A cylindrical biomass pellet, 20 mm tall and 8.2 mm in diameter, was chosen as a sample in this study. The surface of the pellet was slightly glossy, possibly from the pressing process, and the density of the pellet was 1174.0 kg/m^3. An electric heating coil was devised to heat up the biomass pellet located inside the coil, which in turn was mounted inside a coaxial tube for purging the air out with an argon flow. The argon flow was increased until the Raman signal from nitrogen decreased to lower than 5% of the level for ambient air. Under this condition, no oxygen peak was visible in the Raman spectrum, and the pellet did not ignite during the entire heating process. The temperature development at the center of the coil was reproducible for repeated runs and was recorded with a thermocouple prior to the run with the pellet. The values were later used to assign temperatures to the recording times of the data acquired during the pellet pyrolysis. The initial heating rate was 10.7 °C/s for the first 50 s up to 555 °C, where the heating rate starts to decrease, and the temperature then gradually approached 704 °C for the next 280 s. The recording of Raman data started when the heater was switched on.

3. Results and discussion

The PS and PLF methods were implemented with the Raman spectroscopy setup to filter the strong fluorescence signal generated during the biomass pyrolysis. Each image acquired during the biomass experiments first went through the PS process to suppress background from multiple scattered straylight. With these measurements, the PS method was for the first time utilized for applied spectroscopy under challenging conditions in an environment with dense smoke from condensed pyrolysis products. The PS method improved the quality of spectra by suppressing background from multiple scattering, and about 30% of the background level intensity has been removed across the entire wavenumber range through the process. The processed images were then binned into single spectrum vectors and stacked as rows to form the image of Fig. 2a. Therefore, the images of Fig. 2 display wavenumbers and time along the horizontal and vertical axis, respectively. As mentioned previously, temperatures measured during heating without pellet have been assigned to the recording time, as indicated on the right side of Fig. 2a and b. Strong fluorescence from hydrocarbon volatiles covers the entire range of the spectrum during heating at temperatures between 675 and 696 °C, as shown by the broad bright region covering almost the entire width of the image in Fig. 2a. As a result of the PLF procedure, a periodicity in the overall signal intensity was encoded on Raman signals along the y-axis of the spectral image in Fig. 2a, e.g., for nitrogen at 2331 cm^{-1}, and appears as thin horizontal lines across the image. Figure 2b shows the image after filtering using the PLF method. Polarization-independent fluorescence signals have efficiently been filtered out, and therefore more accurate identification of Raman peaks was achieved.

Spectra at three different temperatures from Fig. 2b are selected and compared in Fig. 3, at temperature 688 °C when the fluorescence signal was increasing (a), at 692 °C when the fluorescence was the strongest (b), and at 697 °C when the tar release was about to finish (c). The broad fluorescence of the tars is suppressed by a factor of 25, 15, and 50 in the spectra of Fig. 3a, b, and c, respectively. Moreover, pronounced interference rejection is achieved for two overlapping peaks at wavenumbers 1818 and 1833 cm^{-1}, which for laser excitation at 532 nm are equivalent to wavelengths 589.0 and 589.5 nm, respectively. Intensities of the peaks together with the background dropped by a factor of 40 compared to the input data as a result of the PLF process, cf. Fig. 3a. The filtered peaks are laser-induced atomic emission of sodium (Na) D-lines [24] due to alkali species in the biomass pellets. The suppression of these peaks serves as a good example of filtering polarization-independent signals using the PLF method.

Additional peaks, located at wavenumbers labeled gray in Fig. 3, disappeared after the filtering. Some of them, positioned

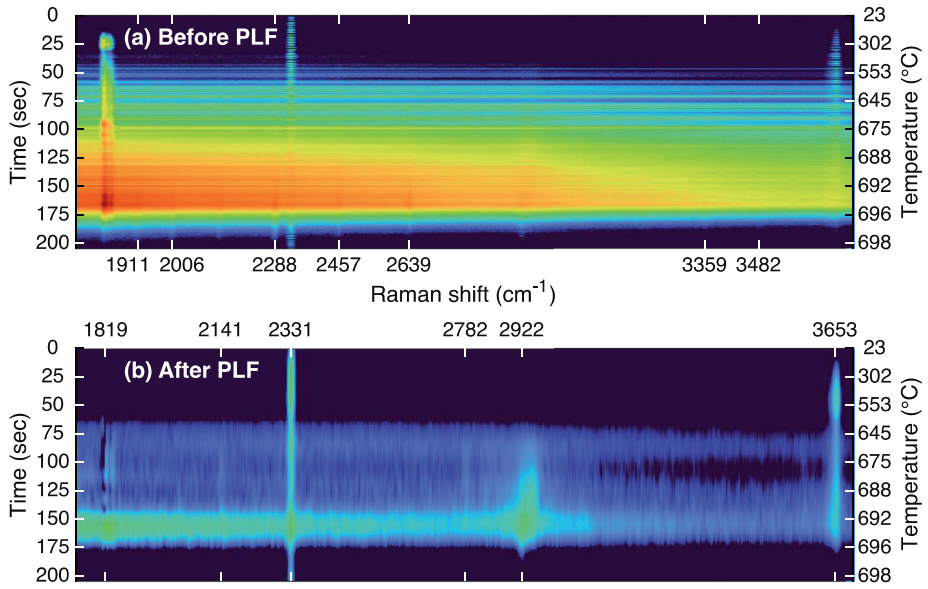

Fig. 2. Images of continuously recorded spectra with temperature increase, (a) before and (b) after polarization lock-in filtering (PLF). The image intensity is presented on a logarithmic scale for clarity. The bright intensity across the entire spectral range in (a) is a background due to fluorescence of hydrocarbon volatiles. This background, as well as some polarization-independent peaks, have efficiently been removed using the PLF filtering in (b).

at wavenumbers 1911, 2006, 2288, 2457, and 2639 cm^{-1}, match the C_2 Swan bands at wavelengths 592.2, 595.6, 605.7, 612.0, and 618.9 nm, respectively [25]. This indicates some photolysis of larger hydrocarbons by the laser. Altogether, the PLF method effectively suppresses fluorescence and laser-induced emission peaks that potentially could be interpreted as false positive Raman signals.

In the spectrum of Fig. 3b, for which the fluorescence contribution was the strongest, a residual fluorescence background of higher intensity at shorter wavenumbers remains after PLF processing, and the spectrum is slightly tilted with a negative slope. In addition to the broad fluorescence contribution of volatiles, the spectrum also shows residual Na peaks at 1881 and 1833 cm^{-1}. Possibly, the release of gases at this stage is too rapid for the PLF method to be able to compensate for the fluorescence background contributions fully. A more rapid modulation might be able to handle this limitation. The residual background was fitted using reference data points where no Raman signal appears, and accounted for in the further quantitative analysis of the Raman peaks.

As a result, Raman signatures of nitrogen, water, hydrocarbons, and carbon monoxide from the biomass pyrolysis were separated from the fluorescence background, and each peak was integrated and converted to an absolute amount using Raman cross-section values obtained from the literature (N_2: 0.46×10^{-30} cm^2/sr, H_2O: 0.9×10^{-30} cm^2/sr, Hydrocarbons: 2.6×10^{-30} cm^2/sr for methane, CO: 0.48×10^{-30} cm^2/sr) [4]. Different classes of hydrocarbons, such as alkanes, oxygenates, and polyaromatic tar compounds, are emitted during pyrolysis [21,22] and contribute to the spectral signature around 2900 cm^{-1}. The composition also varies with time and temperature during the process, which makes the assignment of specific species challenging. Nevertheless, the spectral signature gradually shows a more pronounced peak at 2919 cm^{-1}, indicating increased emission of methane, which is in agreement with the expected trend for the process [21]. Therefore, the cross section of methane was used for the evaluation of the hydrocarbon signal. Since larger hydrocarbons, e.g. higher alkanes, often have higher Raman cross- sections in the CH region [26], the concentration values are likely overestimated. The observed transition of the CH peak indicating a change in the composition of emitted hydrocarbons will be discussed in the last part of this section. Molarities of the species are plotted with time and temperature increase in Fig. 4. As previously mentioned, an argon flow was introduced to prevent the access of oxygen to the pellet during the process, and the amount of nitrogen at the measurement volume while purging was less than 5% of the level in ambient air. The amount of nitrogen under this condition in the probe volume is observed at time 0 in Fig. 4.

In the early stage of heating, the temperature increased at a rate higher than 10 °C/s, and a rapid release of nitrogen and water is observed in Fig. 4. Up to 25 s, nitrogen shows a rapid increase above the initial level at $t = 0$ s due to the release of gas from pores of the pellet. Internal gas storage in the pores of wood biomass under ambient conditions has been confirmed in absorption measurements of oxygen to characterize the porosity of such materials [27]. Between ~25 and 50 s, the nitrogen concentration shows a drop by ~30%, which corresponds to the decrease in molecular number density as the temperature goes up and indicates a rather constant release of nitrogen. The concentration of water increases up to 45 s due to drying of the pellet, and after ~50 s, both nitrogen and water follow a similar decrease up to ~65 s, indicating the end of the first part of the decomposition. After the first stage of the release, the water concentration in the measurement volume gradually increases again, and it is accompanied by the release of hydrocarbons and carbon monoxide. The former is also confirmed by the appearance of the strong fluorescence signal removed in the PLF processing (cf. Fig. 3a). The release of gases continues for around 100 s, after which the concentrations of water, hydrocarbons, and CO have decreased to zero level, while the nitrogen has returned close to its initial value.

As presented in Fig. 3a, the hydrocarbon signature (around 2900 cm^{-1}) is relatively broad, and a further investigation reveals that it is composed of more than one peak, as discussed in the following. The filtered data was used to zoom in on the hydrocarbon peak, which is presented in Fig. 5. The hydrocarbon Raman signal started to appear at 75 s after the heating when the temperature reached 645 °C. At this moment, the peak intensity of the relatively broad spectrum was located at 2944 cm^{-1}. As time passes, temperature increases, and pyrolysis continues, the position of the maximum-intensity started to move toward the shorter wavenum-

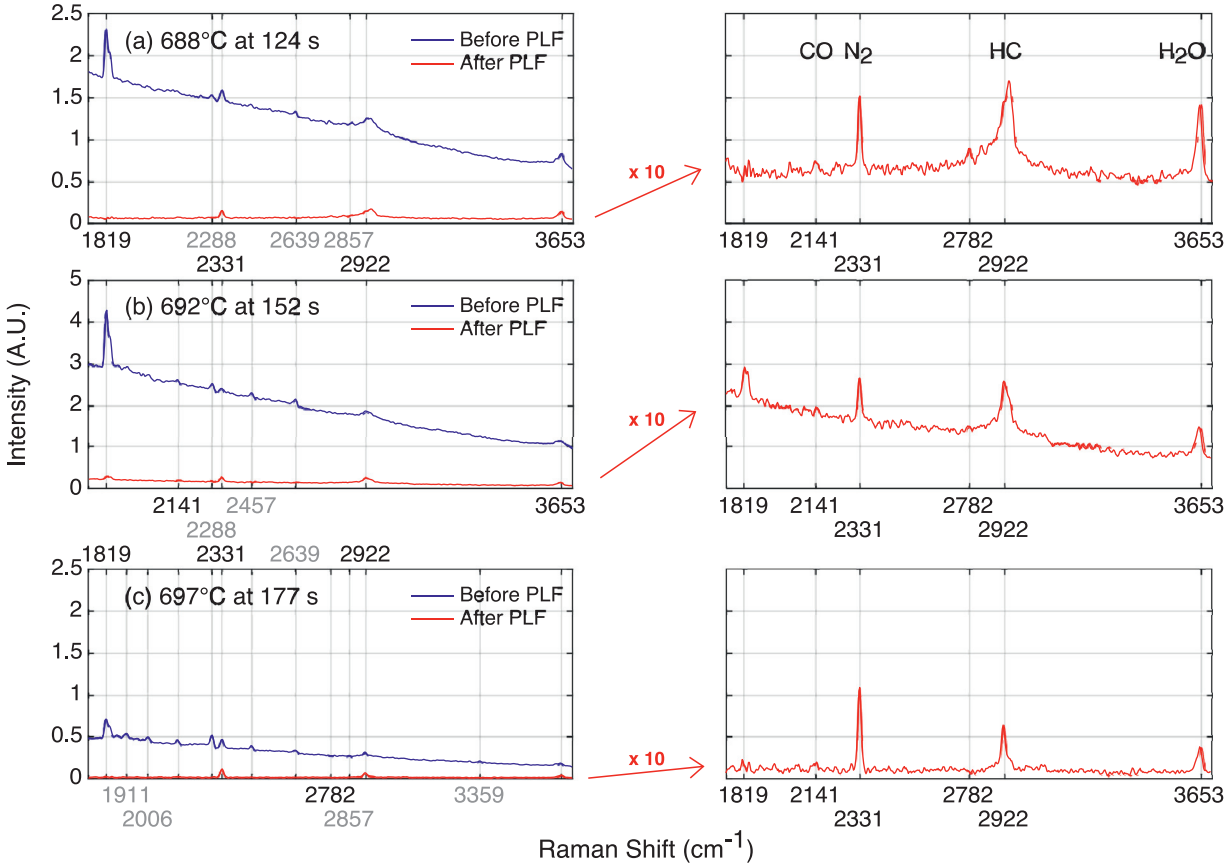

Fig. 3. Spectra of released gas from biomass pyrolysis at a temperature of (a) 688 °C, (b) 692 °C, and (c) 697 °C. The polarization lock-in filtering was utilized to increase the Raman signal-to-background ratio by removing non-Raman signals. Raman peaks of carbon monoxide (CO), nitrogen (N_2), Hydrocarbons (HC), and water (H_2O) are identified.

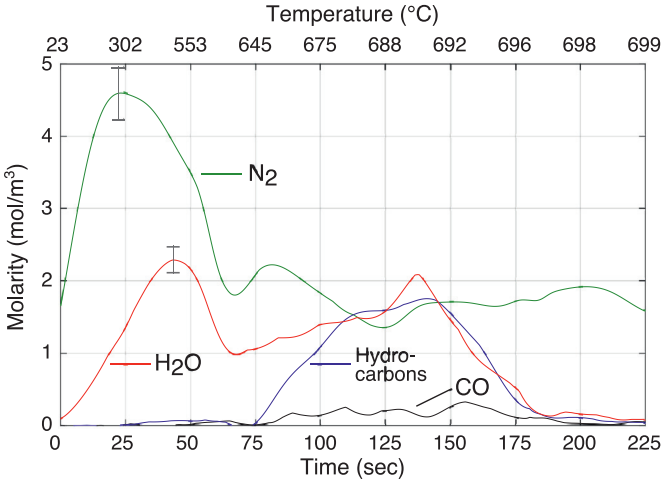

Fig. 4. Absolute amounts of released nitrogen (N_2), water (H_2O), hydrocarbons, and carbon monoxide (CO) during biomass pellet pyrolysis. An argon flow was introduced to the measurement volume to limit the access of oxygen to the biomass pellet. The error bar indicates the range of the largest error in evaluated concentration estimated from repeated Raman concentration measurements in a flame.

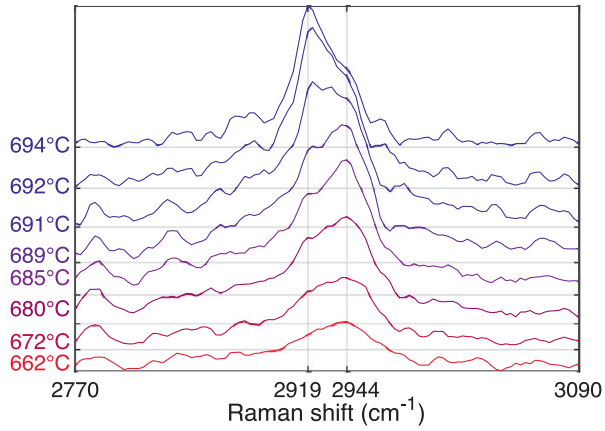

Fig. 5. Change of hydrocarbon Raman spectrum with heating time and temperature increase during pyrolysis. The peak of the hydrocarbon Raman signal located at 2944 cm^{-1} shifts to 2919 cm^{-1} as the process continues. The spectra are plotted with offsets for a better visualization.

ber of 2919 cm^{-1}. After 135 s of heating, when the temperature reached 690 °C, intensities of the two adjacent peaks in the hydrocarbon region were of similar strength. After that, the maximum intensity stayed at 2919 cm^{-1} until the process ended. The initial Raman spectrum located around wavenumber 2944 cm^{-1} suggests that the initial release contains larger hydrocarbons. For example, alkanes and oxygenates, see, e.g., [26,28], reportedly released during the early stages of pyrolysis [21,22]. An additional indication of the release of oxygenated compounds, such as aldehydes, is the appearance of a small peak at 2780 cm^{-1}, suggesting the release of formaldehyde [26], previously also identified in biomass pyrolysis experiments, see, e.g., [29]. Biomass pyrolysis is also accompanied by the release of tars, primarily consisting of polyaromatic hydrocarbons for which Raman spectra often show prominent peaks in the vicinity of 3050 cm^{-1} [30]. However, polyaromatic tars are reported to form at higher temperatures than reached in these experiments [22], and, accordingly, the spectra of Fig. 5 show no ap-

parent features around 3050 cm^{-1}. Considering that the peak at 2919 cm^{-1} can be assigned to methane [26], Raman spectra show a shift of release from heavier hydrocarbons to the lightest one, i.e., methane, in agreement with trends for biomass pyrolysis [21].

4. Conclusions

A polarization lock-in filtering (PLF) method was devised to suppress background interferences on weak Raman scattering signals by temporally modulating signals via the polarization of the excitation laser. The technique was demonstrated for *in situ* analysis of gas released from biomass pyrolysis, which is difficult to achieve with conventional Raman spectroscopy due to the presence of substantial fluorescence interference from volatile larger hydrocarbon compounds. The results are very promising, with suppression of un-polarized background contributions, such as fluorescence and laser-induced atomic emission lines, by up to a factor of 50. The accuracy in identifying the Raman peaks has significantly increased, and concentration evaluation of released species was feasible. Also, the background suppression enables a detailed analysis of spectra, demonstrated by the detection of slight changes in the spectral shape of the hydrocarbon CH-stretch signature.

In addition to the application of biomass pyrolysis presented in this paper, the PLF method can be employed with Raman spectroscopy for measurements under any conditions where the background filtering would be beneficial. While the temporal resolution for time-lapse measurements is primarily set by the laser repetition rate and detector performance, the modulation speed of the laser polarization presently limits the method to studies of processes varying on a time-scale on the order of a second. This can potentially be improved with a faster polarization-switching device, but the technique cannot be employed for single-shot measurements. Nevertheless, the additional complexity of the experimental setup is limited to the addition of a rotating wave plate, and the method thus clearly extends the applicability of Raman spectroscopy setups with a single detection system. Quantitative information is preserved after data post-processing, and including additional factors in the evaluation, e.g., the depolarization ratio of molecules, will increase the accuracy of the quantitative analyses. Therefore, the development of the PLF method will be continued to improve its applicability for optimum use in various fields of research.

Declaration of Competing Interest

The authors declare that they have no known competing financial interests or personal relationships that could have appeared to influence the work reported in this paper.

Acknowledgments

This work was supported by the Swedish Energy Agency project (CECOST 22538-4); the European Research Council (Advanced Grant TUCLA 669466); the Swedish Research Council (VR) (Grant 2015-05321); and the Swedish Foundation for Strategic Research (SSF) (ITM17-0313).

References

[1] M. Lapp, C.M. Penney (Eds.), Laser Raman gas diagnostics, Springer-Verlag U.S., New York, 1974.
[2] W.M. Arden, T.B. Hirschfeld, S.M. Klainer, W.A. Mueller, Studies of gaseous flame combustion products by Raman-spectroscopy, Appl. Spectrosc. 28 (1974) 554–557.
[3] M. Lapp, D.L. Hartley, Raman-scattering studies of combustion, Combust. Sci. Technol. 13 (1976) 199–210.
[4] A.C. Eckbreth, Laser diagnostics for combustion temperature and species, Gordon and Breach, Amsterdam, Netherlands, 1996.
[5] R.A. Hill, D.L. Hartley, Focused, multiple-pass cell for raman-scattering, Appl. Opt. 13 (1974) 186–192.
[6] K.C. Utsav, J.A. Silver, D.C. Hovde, P.L. Varghese, Improved multiple-pass Raman spectrometer, Appl. Opt. 50 (2011) 4805–4816.
[7] K.C. Utsav, P.L. Varghese, Accurate temperature measurements in flames with high spatial resolution using Stokes Raman scattering from nitrogen in a multiple-pass cell, Appl. Opt. 52 (2013) 5007–5021.
[8] Q.V. Nguyen, R.W. Dibble, C.D. Carter, G.J. Fiechtner, R.S. Barlow, Raman-LIF measurements of temperature, major species, OH, and NO in a methane-air Bunsen flame, Combust. Flame 105 (1996) 499–510.
[9] J. Kojima, Q.V. Nguyen, Laser pulse-stretching with multiple optical ring cavities, Appl. Opt. 41 (2002) 6360–6370.
[10] W. Meier, O. Keck, Laser Raman scattering in fuel-rich flames: background levels at different excitation wavelengths, Meas. Sci. Technol. 13 (2002) 741–749.
[11] R.S. Barlow, A.N. Karpetis, Measurements of scalar variance, scalar dissipation, and length scales in turbulent piloted methane/air jet flames, Flow Turbul. Combust. 72 (2004) 427–448.
[12] R.S. Barlow, M.J. Dunn, M.S. Sweeney, S. Hochgreb, Effects of preferential transport in turbulent bluff-body-stabilized lean premixed CH_4/air flames, Combust. Flame 159 (2012) 2563–2575.
[13] G. Magnotti, D. Geyer, R.S. Barlow, Interference free spontaneous Raman spectroscopy for measurements in rich hydrocarbon flames, Proc. Combust. Inst. 35 (2015) 3765–3772.
[14] H. Lee, H. Kim, Y. Lee, Y. Yoon, Jet disintegration in supercritical environments, Exp. Therm. Fluid. Sci. 115 (2020) 110098.
[15] X. Zheng, J. Mantzaras, R. Bombach, Kinetic interactions between hydrogen and carbon monoxide oxidation over platinum, Combust. Flame 161 (2014) 332–346.
[16] E. Kristensson, J. Bood, M. Aldén, E. Nordstrom, J.J. Zhu, S. Huldt, P.E. Bengtsson, H. Nilsson, E. Berrocal, A. Ehn, Stray light suppression in spectroscopy using periodic shadowing, Opt. Express 22 (2014) 7711–7721.
[17] G. Grünefeld, V. Beushausen, P. Andresen, Interference-free uv-laser-induced raman and rayleigh measurements in hydrocarbon combustion using polarization properties, Appl. Phys. B – Lasers Opt. 61 (1995) 473–478.
[18] A. Luczak, V. Beushausen, S. Eisenberg, M. Knapp, H. Schluter, P. Andresen, M. Malobabic, A. Schmidt, New nonintrusive laser diagnostic tools for design and optimization of technically applied combustion systems, Combust. Sci. Technol. 116 (1996) 541–566.
[19] J. Egermann, T. Seeger, A. Leipertz, Application of 266-nm and 355-nm Nd: YAG laser radiation for the investigation of fuel-rich sooting hydrocarbon flames by Raman scattering, Appl. Opt. 43 (2004) 5564–5574.
[20] J.J. Kojima, D.G. Fischer, Multiscalar analyses of high-pressure swirl-stabilized combustion via single-shot dual-Sbg Raman spectroscopy, Combust. Sci. Technol. 185 (2013) 1735–1761.
[21] V. Dhyani, T. Bhaskar, Chapter 9 – pyrolysis of biomass, in: A. Pandey, C. Larroche, C.-G. Dussap, E. Gnansounou, S.K. Khanal, S. Ricke (Eds.), Biofuels: Alternative Feedstocks and Conversion Processes for the Production of Liquid and Gaseous Biofuels, 2nd ed., Academic Press (2019), pp. 217–244.
[22] T.A. Milne, R.J. Evans, N. Abatzaglou, Biomass gasifier "tars": their nature, formation, and conversion, National Renewable Energy Laboratory, Golden, CO (US, 1998 Report No. NREL/TP-570-25357).
[23] M. Israelsson, T.B. Vilches, H. Thunman, Conversion of condensable hydrocarbons in a dual fluidized bed biomass gasifier, Energy Fuel 29 (2015) 6465–6475.
[24] L.P. Granath, C.M. Van Atta, The nuclear spin and magnetic moment of sodium from hyperfine structure, Phys. Rev. 44 (1933) 0935–0942.
[25] A. Gaydon, The spectroscopy of flames, Springer, Dordrecht, Netherlands, 1974.
[26] G. Magnotti, K.C. Utsav, P.L. Varghese, R.S. Barlow, Raman spectra of methane, ethylene, ethane, dimethyl ether, formaldehyde and propane for combustion applications, J. Quant. Spectrosc. Radiat. Transf. 163 (2015) 80–101.
[27] J. Larsson, L. Mei, P. Lundin, J. Bood, S. Svanberg, Development of a compact multipass oxygen sensor used for gas diffusion studies in opaque media, Appl. Opt. 54 (2015) 9772–9778.
[28] G. Dellepiane, J. Overend, Vibrational spectra and assignment of acetone $\alpha\alpha\alpha$ acetone-D3 and acetone-D6, Spectrochim. Acta 22 (1966) 593–614.
[29] C. Brackmann, M. Aldén, P.E. Bengtsson, K.O. Davidsson, J.B.C. Pettersson, Optical and mass spectrometric study of the pyrolysis gas of wood particles, Appl. Spectrosc. 57 (2003) 216–222.
[30] E. Cloutis, P. Szymanski, D. Applin, D. Goltz, Identification and discrimination of polycyclic aromatic hydrocarbons using Raman spectroscopy, Icarus 274 (2016) 211–230.